







Efficiency improvements in a dichroic dye-doped liquid crystal Fresnel lens

ETHAN I. L. JULL,^{1,*}  MARKUS WAHLE,¹  PETER J. M. WYATT,¹  COLIN ELLIS,² STEPHEN J. COWLING,² JOHN W. GOODBY,² KIYOAKI USAMI,³ AND HELEN F. GLEESON¹ 

¹*School of Physics and Astronomy, University of Leeds, LS2 9JT, UK*

²*Department of Chemistry, University of York, Heslington, York YO10 5DD, UK*

³*Osaka Sangyo University, 3-1-1 Nakagaito, Daito-shi, Osaka 574-8530, Japan*

*py12ej@leeds.ac.uk

Abstract: A dichroic dye-doped liquid crystal Fresnel lens was fabricated and investigated to observe the combination of phase and amplitude modulation based focusing. An anthraquinone dichroic dye was doped into a liquid crystal host, which when in the Fresnel lens configuration, generates a Fresnel zone plate with alternating “transparent” and “opaque” zones. The zones were induced by using photo-alignment of a light-sensitive alignment layer to generate the alternating pattern. The voltage dependency of efficiency for the dye-doped and pure liquid crystal Fresnel devices were investigated. Incorporation of dyes into the device yielded a significant 4% improvement in relative efficiency in the lens, giving a maximum of 37% achieved in the device, much closer to the theoretical 41% limit when compared with the non-dye-doped device. The input polarization dependence of efficiency was also investigated, showing very small fluctuations ($\pm 1.5\%$), allowing further insight into the effect of fabrication method on these liquid crystal Fresnel devices.

Published by The Optical Society under the terms of the [Creative Commons Attribution 4.0 License](https://creativecommons.org/licenses/by/4.0/). Further distribution of this work must maintain attribution to the author(s) and the published article's title, journal citation, and DOI.

1. Introduction

The electro-optical properties of liquid crystals [1] (LC) make them incredibly efficient and versatile light manipulators, so that they are ubiquitous in display and non-display technologies. The ease of refractive index modulation, through the application of electric fields (E-field) or external light stimuli, makes them ideal for use in Fresnel technology. The lack of moving parts in LC devices is a clear advantage allowing for simple and direct control of light. Switchable Fresnel lenses are utilised in optical communications, display systems, optical information processing, imaging, and projection. LC Fresnel lens technology has been previously demonstrated through a multitude of methods including; electrode patterning [2–8], polymer-stabilisation [9–14], polymer-relief structures [15–17], polymer-dispersed LCs [18,19], light induced phase effects of azo-doped LCs [20,21], alignment microrubbing [22], UV modification of alignment anchoring strength [23,24], photo-alignment through azo-dopant alignment layer absorption [25–27], and direct substrate photo-alignment [28–33].

The LC Fresnel lens reported here was fabricated using direct substrate photo-alignment [34]. Alternating zones of orthogonal director alignment were created on one surface, which generated the Fresnel pattern, with the other surface treated for homeotropic alignment, Fig. 1(a). This device geometry creates an alternating hybrid aligned nematic (HAN) director field inside the device. Previous dye-doped LC Fresnel lens devices have focused on the use of doped dyes either to generate alternating alignment directions [25–27] or to photo-induce zone specific phase transitions [20,21], and have not investigated their potential impact on efficiency. Use of the dichroic dyes in the LC will generate alternating “opaque” and “transparent” zones which is in

effect a Fresnel zone plate. Fresnel zone plates focus light via amplitude modulation (similar to a standard diffraction grating). However, when considering a dye doped LC Fresnel lens the amplitude modulation focusing will combine with the phase focusing effects of the birefringent material. This report investigates the direct effect of an anthraquinone dichroic dye [35] amplitude modulation based focusing on the efficiency of a switchable dye-doped guest-host LC Fresnel lens.

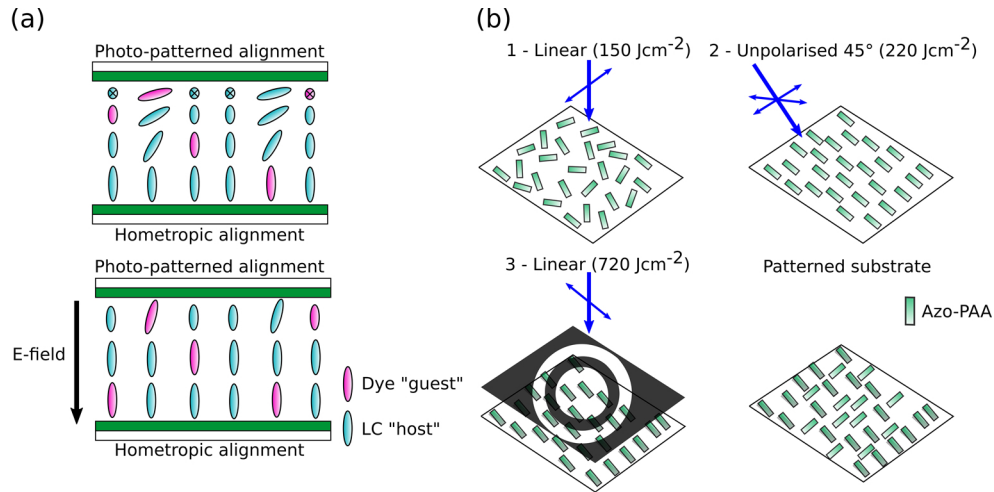


Fig. 1. (a) Schematic of the HAN director field inside the photo-patterned LC Fresnel lens. (b) The photo-patterning process used to generate the Fresnel director pattern in the LC device.

Anthraquinone dichroic dyes have a transition moment approximately parallel to the molecular long axis, which results in a polarization angle dependent absorption. When doped into a LC (host) the dichroic dye (guest) will be oriented by the bulk LC director [36], with the dye long-axis parallel to the director. Therefore, when a LC Fresnel device configuration is considered, a Fresnel zone plate with alternating strongly absorbing and weakly absorbing zones is generated. Fresnel zone plates have a maximum theoretical relative efficiency (ratio of the focused spot intensity to the total transmitted intensity, used commonly in LC Fresnel characterization [4, 10, 16, 19, 20, 23, 25, 30 & 33]) of ~21% (~10.5% absolute efficiency). The light transmitted through this LC Fresnel device will therefore undergo amplitude modulation based focusing due to the alternating absorption caused by the dichroic dye guest-host effect, determined by components of the parallel and perpendicular absorption coefficients, $a_{||}$ and a_{\perp} . Under application of a sufficiently large E-field (the threshold voltage of the device must be exceeded) the director will re-orient and approach the homeotropic (HT) alignment state. This will remove the contrast between zones and the dye absorption will become constant across the device, removing the amplitude-focusing effect. The LC Fresnel device will also focus light due to the inherent birefringence of the LC that causes a phase-shift between alternate zones, $\Phi=2\pi\Delta nd/\lambda$, where Δn is the birefringence, d is the cell gap, and λ the wavelength. The peak in efficiency due to the phase effect occurs when $\Phi=\pi$ (maximum theoretical efficiency ~41%). The refractive index difference between zones can also be controlled via E-field application, and eventually reduced to zero when the device approaches the HT state.

In this report we investigate the coupling of the phase and amplitude modulation focusing effects on the efficiency of this switchable dye-doped LC Fresnel lens.

2. Materials and methods

The LC Fresnel lens described here was fabricated using a masked photo-alignment technique. The photomask was designed with rings of radii; $R_n = \sqrt{n\lambda(f + \frac{n\lambda}{4})}$, where $\lambda=532$ nm, n is the ring number (156 total rings, $R_{\max}=5$ mm), and f the focal point is 0.3 m. A polyamic acid-containing azobenzene in the backbone structure (Azo-PAA, obtained from JNC Petrochemical Co.) [34] was spin coated onto indium tin oxide (ITO) glass before being treated with a 3-step patterning technique, depicted in Fig. 1(b). Initial irradiation of the substrate with linearly polarised light (150 Jcm^{-2}) gives homogenous planar alignment perpendicular to the irradiation polarization. The substrate is then irradiated with unpolarised UV light at 45° incidence angle (220 Jcm^{-2}), inducing a pre-tilt angle of $\sim 2^\circ$. The pre-tilt is induced due to the affinity for the Azo-PAA to orient perpendicular to the UV irradiation polarization. In this case it is unpolarised and therefore results in a preferred orientation into the irradiation direction, more information on this alignment technique can be found in [34]. This step is introduced into the fabrication process to remove defect lines generated by reverse-splay HAN domains which would occur for 0° pre-tilt and cause scattering in the final implementation of the device. Finally, a chrome photomask is placed in contact with the substrate and then irradiated with linear polarised light at 90° to the first irradiation (720 Jcm^{-2}). This generates orthogonal alignment in the photomask transparent zones with a 0° pre-tilt angle. The substrate is then baked at 250°C for 2 hours to fix the alignment. To create the bottom HT aligned substrate, a side-chain-containing AZO-PAA [37] was spin coated onto ITO glass and then baked. The device was then assembled using $50 \mu\text{m}$ spacer film, chosen to give optimal contrast between orthogonal dye doped zones, calculated from 15NB3 guest-host absorption coefficients and the Beer-Lambert law ($a_{//}=0.11\%^{-1}\mu\text{m}^{-1}$ and $a_{\perp}=0.0087\%^{-1}\mu\text{m}^{-1}$).

The LC host chosen for this study was MLC-7023 ($\Delta n = 0.0609$ and $\Delta\epsilon=7.9$) obtained from Merck Chemicals Ltd.. This LC was doped, close to the solubility limit, with 0.50%(w/w) 15NB3 anthraquinone dye ($\lambda_{\max}=540$ nm) synthesized at the University of York [38]. Both pure and dye doped devices were fabricated for direct comparison.

3. Results and discussion

The effective birefringence (Δn_{eff}) for each sample was measured in the HAN device ($\lambda=589$ nm) configuration with varying voltage from 0 to $20 V_{\text{rms}}$ (Fig. 2(a)). For MLC-7023, Δn_{eff} varies from $0.034 \rightarrow 0.001$, whilst 15NB3-doped MLC-7023 has a slightly lower birefringence, varying from $0.031 \rightarrow 0.001$, due to the difference in composition. The measurements of birefringence allow the phase shift in the device to be calculated, allowing a direct comparison of efficiency measurements between samples. The absorption of green laser light ($\lambda=543.5$ nm) polarised parallel and perpendicular to the bulk director ($A_{//}$ and A_{\perp}) was characterized as a function of voltage through use of a photodiode, Fig. 2(b). At $0 V_{\text{rms}}$ $A_{//}=(0.95 \pm 0.02)$ OD, much larger compared to $A_{\perp}=(0.372 \pm 0.005)$ OD. Upon increasing voltage, the contrast in absorption, $\Delta A = A_{//} - A_{\perp}$, decreases as each zone approaches the HT state, going from $\Delta A=(0.57 \pm 0.02)$ OD to $\Delta A=(0.029 \pm 0.001)$ OD. Thus, a continuous reduction in amplitude modulation focusing is generated in the dye doped LC Fresnel lens device.

Polarizing optical microscopy (POM) was used to image the LC Fresnel lens, as shown in Figs. 2(c) and 2(d). Excellent alignment in each device is observed. Figure 2(c) is the MLC-7023 sample viewed between crossed polarisers, with a λ -plate allowing the orthogonal alignment to be observed. Figure 2(d) shows the dye doped sample viewed with a single input polariser, clearly demonstrating the alternating zone absorption effects that are under investigation here. The colour intensity alternates between zones due to orthogonal director alignment.

The focusing efficiency of the device was measured as a function of voltage (0 - $20 V_{\text{rms}}$, frequency = 10 kHz) using an expanded green laser ($\lambda=543.5$ nm, $f_{\text{lens}}=0.29$ m). The relative

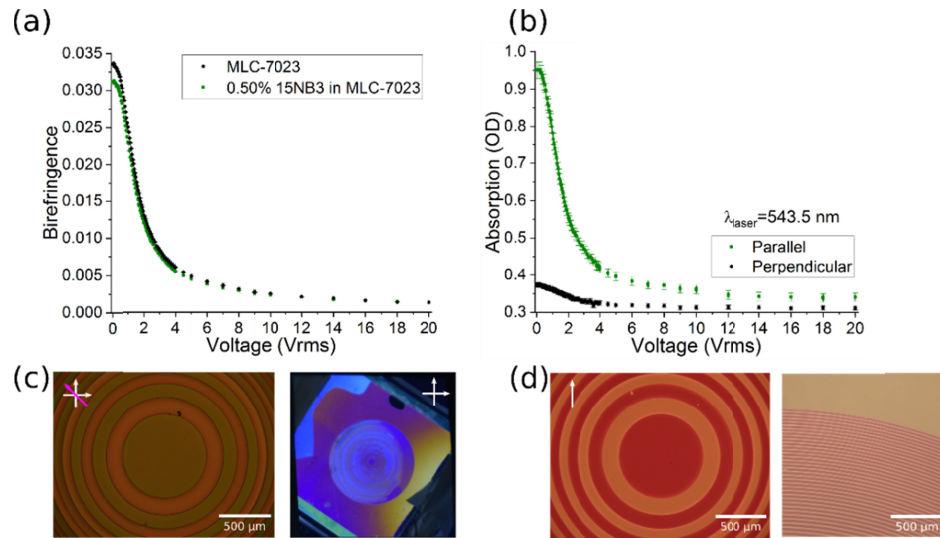


Fig. 2. (a) The birefringence as a function of voltage is shown for MLC-7023 and 15NB3 doped MLC-7023. (b) The absorption of 15NB3 doped MLC-7023 as a function of voltage for parallel and perpendicular light polarisations. (c) POM image showing the LC Fresnel devices MLC-7023 between crossed polarisers with a λ -plate (director(s) at $\pm 45^\circ$). Example device in bulk shown between crossed polarisers. (d) POM image showing the central and radial regions of the LC Fresnel device 15NB3 doped MLC-7023 with a single polariser (director(s) at $0/90^\circ$). All data can be found at <https://doi.org/10.5518/588>.

efficiency (ϵ) is defined as the ratio of the focused spot intensity (I) (measured using a 200 μm pinhole situated at the focal point) to the total intensity transmitted through the device (I_0), $\epsilon = I/I_0$. This definition of diffraction efficiency is commonly used in measuring Fresnel efficiency [4, 10, 16, 19, 20, 23, 25, 30, & 33] and ignores optical reflections or absorption. The absolute efficiency measured in the device will also be demonstrated. The device will exhibit losses with respect to the initial intensity due to dye absorption, and therefore lower absolute efficiency maxima as observed in other amplitude based focusing systems.

To account for the difference in the birefringence of the mixtures (Fig. 2(a)), as well as the small cell gap differences between the devices (50.3 and 50.5 μm), the applied voltage was converted to the equivalent phase shift, $\Phi/\pi = 2\Delta n d/\lambda$, to allow a clear comparison between measurements. The maximum phase focusing efficiency component will theoretically occur when $\Phi = \pi$ ($\Phi/\pi = 1$), with Φ continuously decreasing with increasing voltage. It is noted that the small ($\sim 3\%$) wavelength dispersion and temperature dependence of the LC birefringence will impact the calculated phase shift, and therefore the peak in efficiency vary slightly from $\Phi/\pi = 1$; nonetheless this calculation gives a facile comparison of devices. The amplitude-focusing efficiency component will theoretically start at a maximum at 0 V_{rms} , corresponding to maximum dye contrast, and will then decrease continuously with increasing voltage.

Figure 3(a) shows how the relative efficiency varies with Φ/π for the MLC-7023 and 15NB3 doped MLC-7023 devices (this parameter varies as the applied voltage increases). The dye doped sample provides a 4% increase in efficiency in the phase-focusing states, which correspond to the peaks in efficiency. Away from the phase-focusing states, $\Phi \neq n\pi$, a 3.5% improvement is also observed. The improvements to efficiency are a result of the addition of the amplitude-focusing effects, which are independent of the phase shift. Table 1 demonstrates how these values for efficiency compare with previous literature. Whilst the pure LC Fresnel lens demonstrated here is slightly lower than similar devices (likely due to device imperfections e.g. scattering from zone

boundaries), the dye doped device shows a clear improvement, moving the device towards the top end of currently achieved efficiencies. When comparing devices this close to the maximum theoretical efficiency an improvement of $\sim 4\%$ can provide quite an advantage over other devices. The measured efficiency is lower at low voltages due to the scattering at the zone boundaries where the director field is less ordered at these lower voltages. Figure 3(b) demonstrates the difference between the absolute and relative efficiencies of the dye doped Fresnel device. The absorption caused by the dichroic dye in the system results in a lower overall transmission through the device and therefore a lower absolute efficiency.

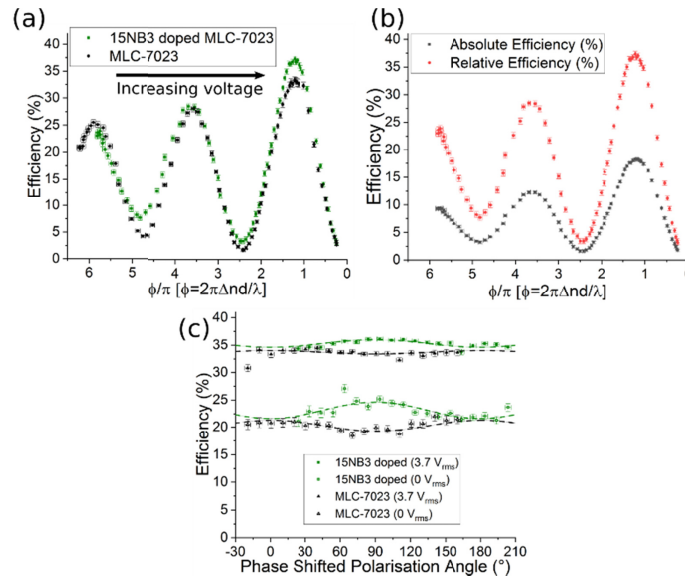


Fig. 3. (a) The relative efficiency as a function of phase shift for MLC-7023 and 15NB3 doped MLC-7023 Fresnel devices. (b) Comparison of absolute and relative efficiency for 15NB3 doped MLC-7023 Fresnel device. (c) The polarization angle dependence of the relative efficiency for each device. 0° corresponds to alignment of the polarization with the “pre-tilted” zone director. Fit parameters can be found in the dataset <https://doi.org/10.5518/588>.

Table 1. Comparison of orthogonal HAN LC Fresnel lens efficiencies.

Maximum efficiency (%)	Reference/Comment
37	This work: (15NB3 doped MLC-7023)
33	This work: (MLC-7023)
34.14	[25] – Orthogonal HAN zones via methyl-red absorption onto surface.
38.5	[28] – Orthogonal HAN zones via masked photo-alignment.
35	[31] – Orthogonal HAN zones via masked photo-alignment.
35	[32] – Orthogonal HAN zones via masked photo-alignment.
34	[33] – Orthogonal HAN zones via photolithography & rubbing.

The polarization angle dependency of this device was thoroughly investigated via efficiency measurements at $0 V_{\text{rms}}$ ($\Phi \neq \pi$) and $3.7 V_{\text{rms}}$ ($\Phi = \pi$) (Fig. 3(c)). Note that 0° polarisation angle corresponds to the alignment of the polarisation of light with the pre-tilted director. Typically, a Fresnel device with orthogonal alignment zones would have polarization independence, however here a small variation in the efficiency of each device with respect to input polarization angle is

measured (maximum $\pm 1.5\%$). This is a direct result of the alignment layer pre-tilt angle ($\sim 2^\circ$) that occurs only in the even zones. The polarization dependence of each device is 90° out of phase with respect to the other, the result of the different types of focal effects (phase or amplitude modulation), each of which is considered here in turn.

In the case of the pure MLC-7023 device at $0 V_{\text{rms}}$ the device is not in the $\Phi=n\pi$ condition, and increases in voltage (decrease in phase-shift/birefringence) increases the efficiency towards the maximum. When the input polarization is at 0° the birefringence between zones is $\Delta n = n_{e,\theta} - n_o$, where $n_{e,\theta}$ is the pre-tilted extraordinary refractive index and n_o is the ordinary refractive index. At 90° the birefringence between zones is simply $\Delta n = n_e - n_o$, where n_e is the extraordinary refractive index. This means that on rotating the input polarisation from 0 to 90° , a small increase in birefringence is observed, moving the device further away from the phase-focusing peak, effectively reducing the efficiency. This can be observed in Fig. 3(c) where the MLC-7023 device efficiency without an applied voltage starts with a maximum value at 0° and decreases slightly to a minimum at 90° . The same effect, although smaller due to the decrease in zone difference under applied voltage, is observed when $3.7 V_{\text{rms}}$ is applied; the shift in birefringence again moves away from the peak in efficiency.

In the case of the 15NB3 doped MLC-7023 device at $0 V_{\text{rms}}$ we have a large difference between $A_{//}$ and A_{\perp} . At 0° input polarization angle there is an effective contrast between zones $\Delta A = A_{\theta} - A_{\perp}$, where A_{θ} is the absorption parallel to the long axis of the pre-tilted director. When the input polarization is at 90° there is an effective contrast between zones of $\Delta A = A_{//} - A_{\perp}$, which is greater than the contrast at 0° . Therefore, on rotation from 0 to 90° we get an increase in absorption contrast and therefore an increase in the amplitude-focusing effect. This can be observed in Fig. 3(c) where the 15NB3 doped MLC-7023 efficiency starts at a minimum at 0° and increases towards a maximum at 90° . The same effect is observed at $3.7 V_{\text{rms}}$, although with a smaller amplitude, again due to the decrease in zone difference under an applied voltage.

4. Conclusion

Development of a dye doped guest-host LC Fresnel lens has been undertaken to investigate the effect of amplitude modulation focusing on the relative efficiency of the Fresnel device. Inclusion of an anthraquinone dichroic dye into the LC host generates a clear improvement in the maximum efficiency of the device from 33 to 37%. Application of a voltage across the device allows the efficiency to be controlled, approaching 0% at voltages $\sim 20 V_{\text{rms}}$, offering a clear variation from focusing to non-focusing. The polarization dependence of the device was investigated and shown to vary due to device pre-tilt, by up to $\pm 1.5\%$ depending on the input polarization angle. This can be attributed to the difference in the pre-tilt alignment of the different zones, and it is noted that the dependency can be removed if device fabrication ensures identical pre-tilt angle between zones.

Funding

Engineering and Physical Sciences Research Council (EP/N509681/1); Daiwa Anglo-Japanese Foundation (11847/12639); Merck Chemicals Ltd..

Acknowledgments

We would like to thank JNC Petrochemical Co. for supplying the polyamic acid solution used in this work.

References

1. J. W. Goodby, P. J. Collings, K. Takashi, C. Tschierske, H. F. Gleeson, and P. Raynes, *Handbook of Liquid Crystals Volume 2: Physical Properties and Phase Behaviour of Liquid Crystals* (Wiley, 2014).

2. G. Li, P. Valley, M. S. Giridhar, D. L. Mathine, G. Meredith, J. N. Haddock, B. Kippelen, and N. Peyghambarian, "Large-aperture switchable thin diffractive lens with interleaved electrode patterns," *Appl. Phys. Lett.* **89**(14), 141120 (2006).
3. G. Li, D. L. Mathine, P. Valley, P. Ayras, J. N. Haddock, M. S. Giridhar, G. Williby, J. Schwiegerling, G. R. Meredith, B. Kippelen, S. Honkanen, and N. Peyghambarian, "Switchable electro-optic diffractive lens with high efficiency for ophthalmic applications," *Proc. Natl. Acad. Sci. U. S. A.* **103**(16), 6100–6104 (2006).
4. W. Hung, Y. Chen, C. Lin, I. Jiang, and T. Hsu, "Sensitive voltage-dependent diffraction of a liquid crystal Fresnel lens," *Appl. Opt.* **48**(11), 2094–2098 (2009).
5. Y. Huang, C. Chen, and Y. Huang, "Superzone Fresnel liquid crystal lens for temporal scanning auto-stereoscopic display," *J. Disp. Technol.* **8**(11), 650–655 (2012).
6. S. Lin, B. Huang, C. Li, K. Yu, J. Chen, and C. Kuo, "Electrically and optically tunable Fresnel lens in a liquid crystal cell with a rewritable photoconductive layer," *Opt. Mater. Express* **6**(7), 2229–2235 (2016).
7. H. Dou, F. Chu, Y. Song, G. Li, and Q. Wang, "A multifunctional blue phase liquid crystal lens based on multi-electrode structure," *Liq. Cryst.* **45**(4), 491–497 (2018).
8. A. Jamali, D. Bryant, Y. Zhang, A. Grunnet-Jepsen, A. Bhowmik, and P. Bos, "Design of a large aperture tunable refractive Fresnel liquid crystal lens," *Appl. Opt.* **57**(7), B10–B19 (2018).
9. N. Rong, Y. Li, Y. Yuan, X. Li, P. Zhou, S. Huang, S. Liu, J. Lu, and Y. Su, "Polymer-stabilized blue-phase liquid-crystal Fresnel lens cured by patterned light using a spatial light modulator," *SID* **47**(1), 1636–1638 (2016).
10. H. Yeh, M. Ke, and Y. Liu, "Electrically switchable Fresnel lenses in polymer-stabilized ferroelectric liquid crystals," *Jpn. J. Appl. Phys.* **56**(1), 012601 (2017).
11. H. Jashnsaz, E. Mohajerani, H. Nemat, S. H. Razavi, and I. A. Alidokht, "Electrically switchable holographic liquid crystal/polymer Fresnel lens using a Michelson interferometer," *Appl. Opt.* **50**(17), 2701–2707 (2011).
12. Y. Fan, H. Ren, and S. Wu, "Switchable Fresnel lens using polymer-stabilized liquid crystals," *Opt. Express* **11**(23), 3080–3086 (2003).
13. N. Avci, Y. Lee, and S. Hwang, "Switchable polarization-independent blue phase liquid crystal Fresnel lens based on phase-separated composite films," *Liq. Cryst.* **44**(7), 1078–1085 (2017).
14. J. Tan, Y. Song, J. Zhu, S. Ni, Y. Wang, Z. Sun, J. Lu, B. Yang, and H. D. Shieh, "Blue phase LC/polymer Fresnel lens fabricated by holographics," *J. Disp. Technol.* **10**(2), 157–161 (2014).
15. M. Wahle, B. Snow, J. Sargent, and J. C. Jones, "Embossing reactive mesogens: A facile approach to polarization-independent liquid crystal devices," *Adv. Opt. Mater.* **7**(2), 1801261 (2019).
16. C. Lee, K. Lo, and T. Mo, "Electrically switchable Fresnel lens based on a liquid crystal film with a polymer relief pattern," *Jpn. J. Appl. Phys.* **46**(7A), 4144–4147 (2007).
17. Y. Fan, H. Ren, and S. Wu, "Electrically switchable Fresnel lens using a polymer-separated composite film," *Opt. Express* **13**(11), 4141–4147 (2005).
18. H. Jashnsaz, N. H. Nataj, E. Mohajerani, and A. Khabbazi, "All-optical switchable holographic Fresnel lens based on azo-dye-doped polymer-dispersed liquid crystals," *Appl. Opt.* **50**(22), 4295–4301 (2011).
19. H. Ren, Y. Fan, and S. Wu, "Tunable Fresnel lens using nanoscale polymer-dispersed liquid crystals," *Appl. Phys. Lett.* **83**(8), 1515–1517 (2003).
20. Y. Kuo and H. Yeh, "Optically controllable transfective Fresnel lens in Azobenzene-doped cholesteric liquid crystals using a Sagnac interferometer," *Appl. Phys. Express* **5**(2), 021701 (2012).
21. H. Yeh, Y. Kuo, S. Lin, J. Lin, T. Mo, and S. Huang, "Optically controllable and focus-tunable Fresnel lens in azo-dye-doped liquid crystals using a Sagnac interferometer," *Opt. Lett.* **36**(8), 1311–1313 (2011).
22. M. Honma and T. Nose, "Liquid-crystal Fresnel zone plate fabricated by microrubbing," *Jpn. J. Appl. Phys.* **44**(1A), 287–290 (2005).
23. S. Hwang, T. Chen, K. Lin, and S. Jeng, "Ultraviolet-light-treated polyimide alignment layers for polarization-independent liquid crystal Fresnel lenses," *Appl. Phys. B: Lasers Opt.* **107**(1), 151–155 (2012).
24. S. Jeng, S. Hwang, J. Horng, and K. Lin, "Electrically switchable liquid crystal Fresnel lens using UV-modified alignment film," *Opt. Express* **18**(25), 26325–26331 (2010).
25. A. Y. Fuh, J. Chen, K. Cheng, and S. Huang, "Polarization-independent and electrically tunable liquid-crystal Fresnel lenses based on photoalignment in dye-doped liquid crystals," *J. Soc. Inf. Disp.* **18**(8), 572–576 (2010).
26. L. Lin, H. Jau, T. Lin, and A. Y. Fuh, "Highly efficient and polarization-independent Fresnel lens based on dye-doped liquid crystal," *Opt. Express* **15**(6), 2900–2906 (2007).
27. T. Lin, Y. Huang, A. Fuh, and S. Wu, "Polarization controllable Fresnel lens using dye-doped liquid crystals," *Opt. Express* **14**(6), 2359–2364 (2006).
28. X. Wang, W. Yang, Z. Liu, W. Duan, W. Hu, Z. Zheng, D. Shen, V. G. Chigrinov, and H. Kwok, "Switchable Fresnel lens based on hybrid photo-aligned dual frequency nematic liquid crystal," *Opt. Mater. Express* **7**(1), 8–15 (2017).
29. X. Wang, A. K. Srivastava, V. G. Chigrinov, and H. Kwok, "Switchable Fresnel lens based on micropatterned alignment," *Opt. Lett.* **38**(11), 1775–1777 (2013).
30. Y. Huang, S. Ko, S. Chu, and A. Y. Fuh, "High-efficiency Fresnel lens fabricated by axially symmetric photoalignment method," *Appl. Opt.* **51**(32), 7739–7744 (2012).
31. D. Kim, S. Lee, and C. Yu, "Electrically controlled diffraction efficiency of liquid crystal Fresnel lens with polarization-independence," *Mol. Cryst. Liq. Cryst.* **476**(1), 133/[379]–140/[386] (2007).

32. D. Kim, C. Yu, H. Kim, S. Kim, and S. Lee, "Polarization-insensitive liquid crystal Fresnel lens of dynamic focusing in an orthogonal binary configuration," *Appl. Phys. Lett.* **88**(20), 203505 (2006).
33. J. S. Patel and K. Rastani, "Electrically controlled polarization-independent liquid-crystal Fresnel lens arrays," *Opt. Lett.* **16**(7), 532–534 (1991).
34. K. Sakamoto, K. Usami, M. Kikegawa, and S. Ushioda, "Alignment of polyamic acid molecules containing azobenzene in the backbone structure: Effects of polarized ultraviolet light irradiation and subsequent thermal imidization," *J. Appl. Phys.* **93**(2), 1039–1043 (2003).
35. M. T. Sims, L. C. Abbott, S. J. Cowling, J. W. Goodby, and J. N. Moore, "Molecular design parameters of Anthraquinone dyes for guest–host liquid-crystal applications: Experimental and computational studies of spectroscopy, structure, and stability," *J. Phys. Chem. C* **120**(20), 11151–11162 (2016).
36. M. T. Sims, "Dyes as guests in ordered systems: current understanding and future directions," *Liq. Cryst.* **43**(13–15), 2363–2374 (2016).
37. K. Usami, K. Sakamoto, J. Yokota, Y. Uehara, and S. Ushioda, "Pretilt angle control of liquid crystal molecules by photoaligned films of azobenzene-containing polyimide with different content of side chain," *J. Appl. Phys.* **104**(11), 113528 (2008).
38. S. J. Cowling, C. Ellis, and J. W. Goodby, "Anthraquinone Liquid crystal dichroic dyes – a new form of chromonic dye?" *Liq. Cryst.* **38**(11–12), 1683–1698 (2011).